

Mechanistic Studies of Substrate-assisted Inhibition of Ubiquitin-activating Enzyme by Adenosine Sulfamate Analogues⁵

Received for publication, July 6, 2011, and in revised form, September 21, 2011. Published, JBC Papers in Press, October 3, 2011, DOI 10.1074/jbc.M111.279984

Jesse J. Chen¹, Christopher A. Tsu, James M. Gavin, Michael A. Milhollen, Frank J. Bruzzese, William D. Mallender, Michael D. Sintchak, Nancy J. Bump, Xiaofeng Yang, Jingya Ma, Huay-Keng Loke, Qing Xu, Ping Li, Neil F. Bence, James E. Brownell, and Lawrence R. Dick

From Discovery, Millennium Pharmaceuticals Inc., Cambridge, Massachusetts 02139

Ubiquitin-activating enzyme (UAE or E1) activates ubiquitin via an adenylate intermediate and catalyzes its transfer to a ubiquitin-conjugating enzyme (E2). MLN4924 is an adenosine sulfamate analogue that was identified as a selective, mechanism-based inhibitor of NEDD8-activating enzyme (NAE), another E1 enzyme, by forming a NEDD8-MLN4924 adduct that tightly binds at the active site of NAE, a novel mechanism termed substrate-assisted inhibition (Brownell, J. E., Sintchak, M. D., Gavin, J. M., Liao, H., Bruzzese, F. J., Bump, N. J., Soucy, T. A., Milhollen, M. A., Yang, X., Burkhardt, A. L., Ma, J., Loke, H. K., Lingaraj, T., Wu, D., Hamman, K. B., Spelman, J. J., Cullis, C. A., Langston, S. P., Vyskocil, S., Sells, T. B., Mallender, W. D., Visiers, I., Li, P., Claiborne, C. F., Rolfe, M., Bolen, J. B., and Dick, L. R. (2010) *Mol. Cell* 37, 102–111). In the present study, substrate-assisted inhibition of human UAE (Ube1) by another adenosine sulfamate analogue, 5'-O-sulfamoyl-N⁶-[(1S)-2,3-dihydro-1H-inden-1-yl]-adenosine (Compound I), a nonselective E1 inhibitor, was characterized. Compound I inhibited UAE-dependent ATP-PP_i exchange activity, caused loss of UAE thioester, and inhibited E1-E2 transthiolation in a dose-dependent manner. Mechanistic studies on Compound I and its purified ubiquitin adduct demonstrate that the proposed substrate-assisted inhibition via covalent adduct formation is entirely consistent with the three-step ubiquitin activation process and that the adduct is formed via nucleophilic attack of UAE thioester by the sulfamate group of Compound I after completion of step 2. Kinetic and affinity analysis of Compound I, MLN4924, and their purified ubiquitin adducts suggest that both the rate of adduct formation and the affinity between the adduct and E1 contribute to the overall potency. Because all E1s are thought to use a similar mechanism to activate their cognate ubiquitin-like proteins, the substrate-assisted inhibition by adenosine sulfamate analogues represents a promising strategy to develop potent and selective E1 inhibitors that can modulate diverse biological pathways.

Post-translational modification by ubiquitin plays an essential role in a wide range of cellular processes. One of the most

intensively studied pathways is the ubiquitin-proteasome system that attaches a polyubiquitin chain to a lysine residue on a target protein and directs it to proteasome-mediated proteolysis. The ubiquitin-proteasome system is a key system responsible for maintaining cellular protein homeostasis, an emerging research area that could potentially transform our understanding of human diseases (1–3). Bortezomib (VELCADE®), a proteasome inhibitor, is currently approved in the treatment of patients with multiple myeloma and relapsed mantle cell lymphoma (4, 5). The clinical success of bortezomib suggests that targeting other components in the ubiquitin-proteasome system pathway might represent an opportunity to develop novel anti-cancer therapeutics (6–9).

Conjugating ubiquitin to a protein substrate is mediated by an enzymatic cascade initiated by ubiquitin-activating enzyme (UAE)² (or Ube1 in humans, also known as E1) (10). Previous mechanistic studies show that, *in vitro*, UAE activates ubiquitin by a three-step process using ATP as a cofactor (Fig. 1A) (11, 12). In step 1, UAE binds ATP and ubiquitin, catalyzes formation of ubiquitin adenylate intermediate, and releases inorganic pyrophosphate (PP_i). The ubiquitin adenylate activates the C-terminal carboxyl group of ubiquitin for nucleophilic substitution. In step 2, the catalytic cysteine residue in UAE attacks the adenylate to form a thioester intermediate (UAE-S~ubiquitin, ~ denotes the thioester bond between the C-terminal carboxyl group of ubiquitin and Cys⁶³² of human UAE) with AMP as the by-product. In step 3, UAE-S~ubiquitin binds another equivalent of ATP and ubiquitin and in a second round of adenylation, forms a UAE-S~ubiquitin-ubiquitin-adenylate ternary complex. Although UAE-S~ubiquitin is capable of transferring ubiquitin to the conjugating enzyme (E2) via a transthiolation reaction, E1-E2 transthiolation is greatly stimulated by occupancy of the nucleotide binding site by either ubiquitin adenylate or ATP alone (13).

⁵The on-line version of this article (available at <http://www.jbc.org>) contains supplemental Table S1 and Figs. S1–S10.

¹To whom correspondence should be addressed: 40 Landsdowne St., Cambridge, MA 02139. Tel.: 617-444-3396; Fax: 617-551-8906; E-mail: jesse.chen@mpi.com.

²The abbreviations used are: UAE, ubiquitin-activating enzyme; NEDD8, neural precursor cell expressed, developmentally down-regulated 8; NAE, NEDD8-activating enzyme; Ubl, ubiquitin-like protein; SPR, surface plasmon resonance; RU, response unit; TLC, thin layer chromatography; ITC, isothermal titration calorimetry; Compound I, 5'-O-sulfamoyl-N⁶-[(1S)-2,3-dihydro-1H-inden-1-yl]-adenosine; Ub-I, ubiquitin-Compound I covalent adduct; Ub-4924, ubiquitin-MLN4924 covalent adduct; UbCH2, human ubiquitin-conjugating enzyme encoded by *UBE2H* gene; UbCH10, human ubiquitin-conjugating enzyme encoded by *UBE2C* gene; DMSO, dimethyl sulfoxide; SUMO, small ubiquitin-like modifier.

Substrate-assisted E1 Inhibition

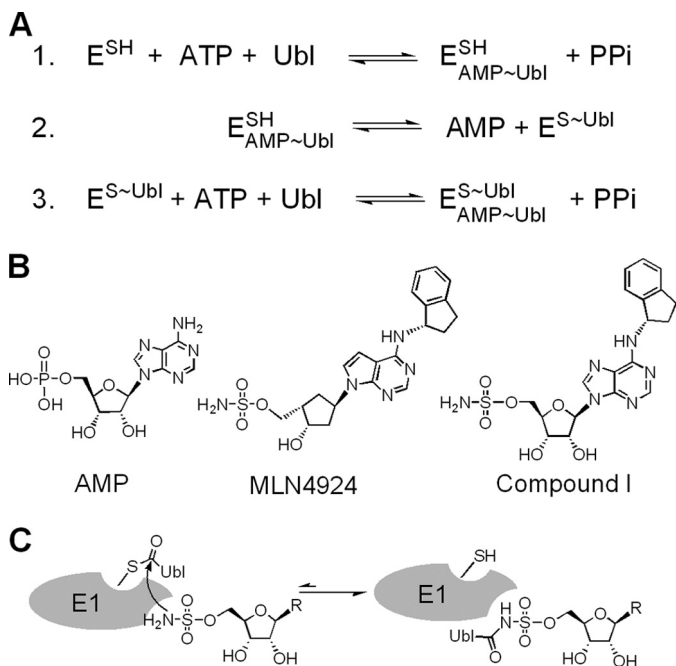


FIGURE 1. **Proposed mechanisms of Ubl activation and E1 inhibition.** A, three-step Ubl activation leading to a ternary complex via a Ubl-adenylate intermediate. B, structures of AMP and two adenosine sulfamate analogues, MLN4924 and Compound I. C, proposed mechanism of E1 inhibition by adenosine sulfamates.

In humans, eight E1 enzymes and more than a dozen ubiquitin-like protein (Ubls) have been identified that play important roles in regulating diverse biological pathways (10). Members of the E1 enzyme class share common sequence and structural features and all use a similar mechanism involving adenylation and thioester formation (14). Besides ubiquitin, another extensively studied Ubl-conjugation pathway involves NEDD8 (Rub1 in yeast), a Ubl that shares ~60% sequence similarity with ubiquitin (15, 16). Like ubiquitin, NEDD8 is activated via an adenylation intermediate by an E1 known as NEDD8-activating enzyme (NAE), which then transfers NEDD8 to an E2 (Ubc12 or Ube2M in humans) (17). Recently, we described MLN4924 (Fig. 1B), a potent and selective inhibitor of NAE that is currently being evaluated in Phase I clinical trials (18–20). MLN4924 is a mechanism-based NAE inhibitor that forms a covalent NEDD8-MLN4924 adduct, a novel mechanism termed substrate-assisted inhibition (21). Biochemical studies demonstrated that formation of the NEDD8-MLN4924 adduct is strictly ATP-dependent and requires the catalytic cysteine, which leads to the hypothesis that the adduct is formed via nucleophilic attack of the NAE-S~NEDD8 thioester by the sulfamate group of MLN4924 after completion of step 2 (Fig. 1C). The covalent adduct mimics the NEDD8-adenylate intermediate and binds at the adenylation site of NAE to form a tight binary complex, which inhibits the ability of NAE to bind NEDD8 or ATP (21).

Because all E1s are thought to utilize similar mechanisms to activate their cognate Ubls (10, 14), the substrate-assisted NAE inhibition demonstrated by MLN4924 could potentially represent a general strategy to develop selective inhibitors against other E1s. Indeed, one such adenosine sulfamate analogue, Compound I (Fig. 1B), was shown to form Ubl-adducts with a

panel of E1s (21). In this study, we describe detailed mechanistic studies of Compound I-mediated UAE inhibition and present biochemical evidence to support the proposed substrate-assisted inhibition mechanism using the purified Compound I-ubiquitin adduct. In addition, pre-steady-state kinetic analysis has been performed to directly obtain kinetic parameters of the adduct-forming reaction catalyzed by UAE. Inhibition and affinity studies were also conducted with MLN4924, a weak UAE inhibitor, and its ubiquitin adduct. The results indicate that both adduct formation and its affinity to E1 contribute to potency of E1 inhibition mediated by adenosine sulfamate analogues.

EXPERIMENTAL PROCEDURES

Materials— $[^{32}P]PP_i$ (catalog number NEX019), $[\alpha\text{-}^{32}P]ATP$ (catalog number BLU003H250UC), and $[\gamma\text{-}^{32}P]ATP$ (catalog number BLU002250UC) were obtained from PerkinElmer Life Sciences. $[^3H]AMP$ was purchased from American Radiolabeled Chemicals, Inc. (St. Louis, MO, catalog number ART1556). Bovine ubiquitin (catalog number U6253), rabbit muscle pyruvate kinase Type III (catalog number P0072), and rabbit muscle myokinase (catalog number M3003) were purchased from Sigma. Rabbit muscle lactate dehydrogenase was purchased from Calbiochem (catalog number 427217). N-terminal FLAG-tagged ubiquitin with the sequence of N-MDYKDDDDK-ubiquitin_{2–76} was generated by gene synthesis and subcloning in a pDEST14 vector and expressed in *Escherichia coli*. Mouse monoclonal anti-FLAG M2 antibody was purchased from Sigma (catalog number F1804). Mouse monoclonal anti-ubiquitin antibody (P4D1) and anti-tubulin antibody were purchased from Santa Cruz Biotechnology (catalog numbers sc-8017 and sc-23948, respectively). Rabbit polyclonal anti-UbcH10 antibody was purchased from Boston Biochem Inc., Cambridge, MA (catalog number A-650). Rabbit monoclonal anti-Compound I antibody was generated in-house using a method described in previous studies (18, 21). Other chemicals were purchased from Sigma. N-terminal His₆-tagged human Ube1 (UAE, wild-type and C632A mutant) and other E1s were expressed in Sf9 insect cells and purified as described before (18, 22). N-terminal glutathione S-transferase (GST)-tagged UAE or UbcH2 fusion protein and untagged UbcH10 were expressed in *E. coli*. Expressed proteins were purified by affinity or conventional chromatography using standard buffers.

Purification of Ubiquitin-Compound I (Ub-I) and Ubiquitin-MLN4924 (Ub-4924) Adduct—A typical reaction mixture of 1 ml contained 12 μM UAE, 10 μM ubiquitin, 50 μM Compound I or MLN4924, 250 μM ATP, and 10 mM $MgCl_2$ in 50 mM Tris-HCl, pH 7.5. The reaction mixture was incubated at room temperature for 30 min and quenched with addition of 100 μl of 0.5 M EDTA, pH 8.0. A reverse-phase HPLC system was developed to purify the ubiquitin-inhibitor adduct from the crude reaction mixture using a Proto300 C4 (300 Å, 5 μm , 2.1 \times 100 mm, Higgins Analytical, Mountain View, CA, catalog number RS-1021-W045). The elution system utilized 0.1% formic acid/water as Buffer A and 0.1% formic acid in 90:10 water/acetonitrile as Buffer B. The elution was performed using a gradient of 20% B from 0 to 5 min followed by 20% B to 60% B from 5 to 25

min with a flow rate of 0.3 ml/min (retention time: ubiquitin, 14.9 min; Ub-I, 15.7 min; Ub-4924, 15.7 min). The fractions containing ubiquitin-inhibitor adducts were pooled and co-evaporated with water 3 times *in vacuo* to remove organic solvent. The final samples were re-dissolved in 20 mM HEPES, pH 7.5. The concentration of ubiquitin adduct was determined using UV absorption at 280 nm with calculated extinction coefficients based on ϵ_{280} values of ubiquitin and inhibitors (ϵ_{280} for Ub-I: 15.7 $\text{mM}^{-1} \text{cm}^{-1}$; for Ub-4924, 15.2 $\text{mM}^{-1} \text{cm}^{-1}$). The average overall yields were ~ 60 –70%. The identity of the purified adduct samples was confirmed by LC/MS analysis (m/z for $[M + H]^+$: Ub-I, calculated, 9009.38, observed, 9009.80; Ub-4924, calculated, 8990.42, observed, 8991.31).

ATP-PP_i Exchange Assay—The ATP-PP_i exchange assay was performed using an improved protocol developed by Bruzzese *et al.* (22). For potency measurement, inhibitors were serially diluted into a 96-well assay plate and a mixture containing 0.5 nM wild-type UAE or UAE mutant (C632A), 0.01, 0.1, or 1 mM ATP, and 0.1 mM PP_i (containing 50 cpm/pmol of [³²P]PP_i) in 1× E1 buffer (50 mM HEPES (pH 7.5), 25 mM NaCl, 10 mM MgCl₂, 0.05% BSA, 0.01% Tween 20, and 1 mM DTT) was added. Reactions were initiated by adding ubiquitin (final concentration: 1 μM) and were incubated for 60 min at 37 °C before quenching with 5% (w/v) trichloroacetic acid (TCA) containing 10 mM PP_i. The quenched reaction mixtures were transferred to a Dot-Blot System (Whatman, catalog number 10447900) loaded with activated charcoal filter paper, washed, and quantitated on a phosphorimager (Fujifilm FLA-7000, GE Healthcare) as described previously (22). The spot intensities were converted to the amount of ATP using a standard curve generated with [α -³²P]ATP (22). Inhibition studies of other E1s by Compound I were performed with their cognate UbIs using similar procedures as described above. Time-dependent inhibition of the ATP-PP_i exchange activity by UAE was performed under similar conditions except that at each time point, an aliquot of reaction mixture was quenched with 5% (w/v) TCA containing 10 mM PP_i and was transferred onto charcoal filter paper for the quantitation of radioactive ATP produced in the reaction. The data were fitted using the slow, tight-binding kinetic model described by Morrison and Walsh (23).

E1-E2 Transthioylation Assays—Time-resolved fluorescence resonance energy transfer was used to quantitate the amount of UbCH2-S~ubiquitin catalyzed by UAE following a similar protocol developed for NAE activity measurement (18). The inhibitor potency assay mixture contained 0.35 nM UAE, 35 nM N-FLAG-ubiquitin, 8 nM GST-UbCH2, 2.5 mM MgCl₂, and 75 nM ATP in 50 mM HEPES, pH 7.5, and 0.05% BSA with inhibitors in a 3× dilution series. The reaction mixtures were incubated in a solid white 384-well microtiter plate at 37 °C for 90 min before being quenched with 20 mM EDTA. The quenched samples (50 μl) were then mixed with 25 μl of the detection solution containing 0.6 nM anti-FLAG europium cryptate (Cisbio, Bedford, MA, catalog number 61FG2KLB), 8.1 $\mu\text{g}/\text{ml}$ of anti-GST-allophycocyanin (Prozyme, Hayward, CA, catalog number PJ252p1), and 0.4 M potassium fluoride (in 50 mM HEPES, pH 7.5, and 0.05% BSA). The reaction mixtures were incubated for 2 h at room temperature and time-resolved fluorescence resonance energy transfer was measured on a

PHERASTAR *plus* instrument equipped with an HTRF® optical module (BMG Labtech, Offenburg, Germany).

The steady-state rate of E1-E2 transthioylation was measured by quantitating AMP production using a coupled assay with an ADP-ATP cycling system (24). A typical reaction mixture (2 ml) contained 0.5 nM UAE, 4 μM ubiquitin, 1 μM UbCH10, 100 μM ATP, 10 units/ml of rabbit muscle myokinase, 20 units/ml of rabbit muscle pyruvate kinase, 50 units/ml of rabbit muscle lactate dehydrogenase, 1 mM phosphoenolpyruvate, 3.4 μM NADH in 5 mM MgCl₂, 25 mM NaCl, 50 mM HEPES, pH 7.5. The reaction mixture was incubated at 37 °C and the loss of NADH fluorescence was monitored on a Cary Eclipse Fluorimeter (Varian Inc., Mulgrave, Victoria, Australia), with the following instrument settings: λ_{ex} , 350 nm; λ_{em} , 460 nm; slits, 20 nm; filter, auto; PMT, 650; cycle, 2 s; and read, 0.1 s. The fluorescence signal loss due to NADH reduction was converted to the amount of AMP produced in the reaction mixture using a standard curve. Time-dependent inhibition of E1-E2 transthioylation was measured in the presence of 50–300 nM Compound I. For each Compound I concentration, the observed rate of inhibition (k_{obs}) was derived by fitting the progress curve with a slow, tight-binding kinetic model (23).

UAE-S~Ubiquitin Thioester Inhibition Assay—The reaction mixture (50 μl) contained 1 μM N-FLAG-ubiquitin, 50 nM UAE, 0.1 or 1 mM ATP, 10 mM MgCl₂ in 1× E1 buffer with Compound I in a 3× dilution series (in 1 μl of DMSO, top concentration of 100 μM , total 10 concentrations). The reaction mixture without UAE was first mixed with Compound I in a 96-well plate and UAE was added to initiate the reaction. The plate was incubated at room temperature for 15 min and quenched with 4× LDS sample loading buffer (Invitrogen, catalog number NP0007). The quenched samples were analyzed by SDS-PAGE under nonreducing conditions, transferred to 0.2- μm Immobilon-P PVDF membrane (Millipore, catalog number ISEQ20200), and probed with either anti-FLAG or anti-Compound I antibody. Alexa Fluor 680-labeled secondary antibody (Invitrogen, catalog number A21109 for anti-rabbit and A21057 for anti-mouse) was then used and quantitation of protein bands was performed on a Li-Cor Odyssey Imaging System (Li-Cor Biosciences, Lincoln, NE).

Quantitation of AMP and PP_i by Thin Layer Chromatography (TLC)—To quantitate the amount of ubiquitin adenylate or AMP generated in the UAE-catalyzed ubiquitin activation reaction, 5 μM ubiquitin was mixed with 1 μM UAE in a mixture containing 25 μM ATP, [α -³²P]ATP (1 $\mu\text{Ci}/\text{nmol}$), 10 mM MgCl₂, and 50 mM Tris, pH 7.5. The reaction mixture was incubated at room temperature for 5 min and quenched by adding 0.5 M EDTA. The reaction mixture (1 μl) was then spotted on a PEI-TLC plate (J. T. Baker, Inc., Phillipsburg, NJ, catalog number 4474-04) that was pre-run with water and eluted with 1 M LiCl. Under this condition, ubiquitin adenylate was shown to be completely hydrolyzed to ubiquitin and AMP (data not shown). To quantitate the amount of PP_i generated in the reaction, a similar reaction mixture was prepared as described above except that [γ -³²P]ATP (1 $\mu\text{Ci}/\text{nmol}$) was used instead of [α -³²P]ATP. The reaction mixture was quenched by adding 0.5 M EDTA and eluted on a PEI-TLC plate with 0.75 M KH₂PO₄, 4 M urea, pH 3.5. The PEI-TLC plate was air dried and exposed to

Substrate-assisted E1 Inhibition

an imaging plate for 1 h before being visualized and analyzed using the phosphorimager. The amount of AMP or PP_i produced in the reaction was determined from the ratios of spot intensities between AMP or PP_i and the remaining ATP.

ATP-AMP Exchange Assay—The reaction mixture contained 1.2 μM ubiquitin, 1 mM ATP, 1 mM AMP, 0.2 μCi/nmol of [³H]AMP, 10 μM PP_i, 200 nM UAE in 10 mM MgCl₂, 0.1 mM DTT, and 50 mM Tris-HCl, pH 7.5. The reaction mixture without ubiquitin was first mixed with Compound I in a 3× dilution series (in 1 μl of DMSO, top concentration of 100 μM, total 10 concentrations) in a 96-well plate and ubiquitin was added to initiate the reaction. The reaction mixture was incubated at 37 °C for 20 min before being quenched by 0.5 M EDTA, pH 8.0. The reaction mixture (1 μl) was then spotted on a PEI-TLC plate that was pre-run with water and eluted with 1 M LiCl. The PEI-TLC plate was air dried and exposed to a high-sensitivity imaging plate for 48 h before being visualized and analyzed using the phosphorimager.

Pre-steady-state Kinetic Studies—Pre-steady-state kinetic experiments were performed at 37 °C on a rapid chemical quench apparatus manufactured by Kintek (Model RQF-3, Kintek, State College, PA). To measure the rate of Ub-I formation, pre-formed UAE-S~ubiquitin was used. To prepare UAE-S~ubiquitin, 13 μM UAE was mixed with 10 μM ubiquitin in a total volume of 300 μl containing 50 μM ATP, 5 mM MgCl₂, and 20 mM HEPES, pH 7.5. The reaction mixture was incubated at room temperature for 10 min and loaded onto a PD MiniTrap G25 desalting column (GE Healthcare) pre-equilibrated with 1× E1 buffer. The final elution volume was 1.5 ml with an expected UAE-S~ubiquitin concentration of 2 μM. To initiate the reaction, 20 μl of 2 μM UAE-S~ubiquitin in Syringe A was rapidly mixed with 20 μl of 20, 40, 60, 80, 120, or 160 μM Compound I in Syringe B at 37 °C. At various time points ranging from 50 ms to 1.5 s, the reaction was quenched with 1 N HCl. The quenched reaction mixture was then analyzed by SDS-PAGE followed by Western blotting with anti-Compound I antibody. The intensity of the adduct bands were quantitated on a Li-Cor Odyssey Imaging System using a standard curve obtained from purified Ub-I samples (3–400 fmol). Samples from each time point were analyzed in duplicate.

To measure the rate of ubiquitin adenylate formation (step 1), 20 μl of a solution containing UAE, ATP, and [α-³²P]ATP in Syringe A was rapidly mixed with 20 μl of a solution containing ubiquitin in Syringe B on the Kintek RQF-3 apparatus at 37 °C. The final reaction mixture contained 2.5 μM UAE, 2 μM ubiquitin, 12.5, 25, or 50 μM ATP in 10 mM MgCl₂, and 50 mM HEPES, pH 7.5. At 10, 20, 30, 40, 50, 60, 80, 100, 150 ms, the reaction was quenched with 1 M HCl. The quenched solution (10 μl) was then mixed with 40 μl of 0.5 M EDTA, from which 1 μl was spotted on a PEI-TLC plate, eluted with 1 M LiCl, and analyzed using the phosphorimager as described before. Samples from each time point were analyzed in triplicate.

To measure the rate of UAE-S~ubiquitin formation, 20 μl of a solution containing UAE and ATP in Syringe A was rapidly mixed with 20 μl of a solution containing ubiquitin in Syringe B on the Kintek RQF-3 apparatus at 37 °C. The final reaction mixture contained 1.5 μM UAE, 1 μM ubiquitin, 500 μM ATP in 10 mM MgCl₂, and 50 mM HEPES, pH 7.5. At various time points

ranging from 50 ms to 2 s, the reaction mixture was quenched with 1 N HCl and analyzed by Western blot on a Li-Cor Odyssey Imaging System as described in the UAE thioester inhibition assay. Samples from each time point were analyzed in triplicate.

Surface Plasmon Resonance (SPR) Experiments—All SPR experiments were performed on a Biacore S51 instrument (GE Healthcare). N-terminal GST-tagged UAE was immobilized on a sensor chip surface using the anti-GST antibody capturing method. Goat polyclonal anti-GST antibody was covalently attached to a carboxymethyl dextran-coated sensor chip surface (CM5 from GE Healthcare, catalog number BR-1006-68) using the amine-coupling protocol provided by the manufacturer (GE Healthcare, catalog number BR-1006-33). Briefly, the carboxymethyl groups on the blank CM5 chip surface were first reacted with *N*-ethyl-*N'*-(3-dimethylaminopropyl)carbodiimide and *N*-hydroxysuccinimide. Goat polyclonal anti-GST antibody (30 μg/ml, catalog number BR-1002-23, GE Healthcare) was then injected onto the activated sensor chip surface at a flow rate of 10 μl/min in 10 mM sodium acetate, pH 5.0, for 10 min. The sensor chip surface was then blocked with ethanolamine. The level of immobilization was typically ~12,000–13,000 response units (RU, 1 RU represents binding of ~1 pg of protein/mm² on the sensor chip surface). N-GST-UAE (10 μg/ml) was then captured on the sample spot with a capture level of ~900–1200 RU (flow rate: 30 μl/min). Purified recombinant GST (5 μg/ml) was captured on the control spot with a capture level of ~1200 RU. The SPR data were collected at 25 °C with a flow rate of 90 μl/min in a sample running buffer containing 10 mM HEPES (pH 7.5), 150 mM NaCl, 0.005% P-20 (as surfactant), and 0.1 mg/ml of BSA. All data acquisition (in duplicate) and subsequent analysis were performed with recombinant GST as the control. The kinetics of association and dissociation data were fit with a single exponential rise or decay equation. The equilibrium affinity binding data were fit using a one-site binding model.

Binding Affinity Measurement Using Isothermal Titration Calorimetry (ITC)—The affinity between UAE and ubiquitin was measured by ITC using an Auto-iTC₂₀₀ microcalorimeter (Micro-Cal Inc., a subsidiary of GE Healthcare) controlled by VPViewer software. All samples were prepared in the same buffer (20 mM NaCl, 1 mM tricarboxyethyl phosphine in 20 mM HEPES, pH 7.5) and were thoroughly degassed by being stirred under vacuum before use. ITC experiments were performed at 25 °C using a reference power of 10 μcal/s. The sample cell (0.2 ml) contained 20–25 μM UAE, which was titrated against 500–550 μM ubiquitin (injectant) in 1.4-μl volumes. The syringe speed was set at 1000 rpm. The affinity between UAE and Compound I was measured in a similar procedure. Experiments were either terminated after saturation or left to continue until all 28 programmed injections had occurred. The ITC data were corrected for the heat of dilution of the injectant by subtracting the control experiments (ubiquitin titrated against buffer) for each titration. The corrected data were analyzed with Microcal Origin 7.0, and the fitting curves were calculated according to a one-site binding model. Experiments were performed in triplicate to confirm constant calculations.

UAE Activity Recovery Assay—The recovery of the activity of UAE was monitored using a similar procedure as described for

the E1-E2 transthiolation assay using time-resolved fluorescence resonance energy transfer. UAE-inhibitor complexes (1 μM), which were formed by incubating UAE with Compound I/ubiquitin/ATP, were diluted 1:50,000 (~ 20 pM UAE final concentration) into UbcH2 transthiolation reaction mixtures as described above except that the concentration of ATP was 3 mM. The reaction mixtures were incubated at 37 °C. An aliquot was removed at various time points and quenched with 20 mM EDTA. The quenched samples were then transferred to a solid white 384-well microtiter plate, mixed with the detection solution, and analyzed on a PHERAstar *plus* instrument as described above.

Time Course Analysis of Ub-4924 Formation—The reaction mixture contained 1 μM ubiquitin, 40 nM UAE, 250 μM ATP, 50 μM MLN4924, 5 mM MgCl_2 , in 50 mM HEPES, pH 7.5. The reaction mixture was incubated at 37 °C. An aliquot of 80 μl was removed at 0, 0.5, 1, 2, 3, and 4 h, quenched with 5 μl of 0.5 M EDTA and 20 μl of acetonitrile, and analyzed by reverse phase-HPLC under similar conditions as described for adduct purification.

Cellular Assays to Study Inhibition of the UAE Pathway—The cellular studies to assess the pathway inhibition by Compound I were performed using the HCT116 cell line as described before (18, 21). Briefly, cells were treated with either 0.1% DMSO (negative control) or 10 μM Compound I for 1 h. Cells were then harvested and washed with cold PBS solution. The cells were then lysed and the whole cell extracts were prepared and normalized by total protein concentration. The samples containing 40 μg of protein were then separated by SDS-PAGE under nonreducing conditions and transferred to nitrocellulose membrane as described above. The membrane was then probed with anti-UbcH10, anti-ubiquitin, or anti-tubulin antibodies.

RESULTS

Inhibition of the ATP-PP_i Exchange Activity of UAE—Compound I was identified as an inhibitor against a panel of recombinant human E1s including UAE (21). Further mass spectrometry analysis revealed a species in the E1 inhibition reaction mixture that was consistent with a covalent, Ubl-Compound I adduct, similar to the NEDD8-MLN4924 adduct observed previously (21). In the present study, Compound I was shown to be a potent inhibitor against wild-type UAE in ATP-PP_i exchange assays (Fig. 2A, filled circles). The IC₅₀ values ranged from 10.2 nM to 5 μM with an increasing ATP concentration from 10 μM to 1 mM, suggesting that the inhibition by Compound I is ATP competitive (Table 1). Compound I did not inhibit UAE with a C632A mutation that prevents UAE-S~ubiquitin thioester formation (Fig. 2B). The absolute requirement of ATP and an intact Cys⁶³² residue for inhibition are consistent with the proposed reaction between UAE-S~ubiquitin and Compound I as the necessary step leading to UAE inhibition (Fig. 1C). In addition, ATP is expected to compete with Compound I in binding to UAE-S~ubiquitin (step 3 in Fig. 1A), which is consistent with the observed ATP competitiveness of UAE inhibition by Compound I (Table 1). In addition to UAE, Compound I also demonstrated varying degrees of potency against other recombinant human E1s in ATP-PP_i exchange assays (supplemental

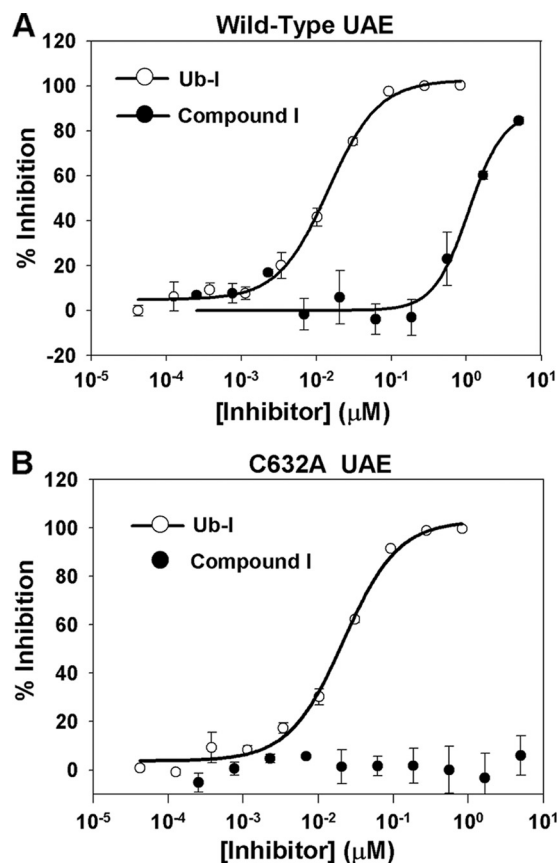


FIGURE 2. Inhibition of UAE by Compound I or Ub-I using the ATP-PP_i exchange assay. A, wild-type UAE. B, C632A UAE. The assay mixtures contained 1 mM ATP. Results are summarized in Table 1.

TABLE 1

Summary of IC₅₀ values for UAE inhibition by Compound I or Ub-I with different ATP concentrations

Data with 1 mM ATP are derived from Fig. 2.

	IC ₅₀		
	10 μM ATP	100 μM ATP	1 mM ATP
Compound I	10.2 \pm 1.7	^{nm} 90.8 \pm 9.8	5.21 $\times 10^3$
Ub-I	1.1 \pm 0.1	5.0 \pm 0.5	14.4 \pm 1.4
Ub-I (C632A UAE)	0.89 \pm 0.04	2.9 \pm 0.1	21.7 \pm 0.3

Table S1), suggesting that unlike MLN4924, Compound I is a nonselective E1 inhibitor.

To confirm that the covalent, ubiquitin-Compound I adduct (Ub-I) is the species directly responsible for UAE inhibition, we attempted to isolate Ub-I from the enzymatic reaction mixture containing UAE, Mg^{2+} -ATP, ubiquitin, and Compound I. With an excess amount of UAE, ubiquitin was quantitatively converted to Ub-I, which was purified from the reaction mixture by reverse-phase HPLC (supplemental Fig. S1). Ub-I is a potent inhibitor of UAE and its inhibition is also ATP-competitive (Fig. 2A, open circles, and Table 1). With the same ATP concentration, IC₅₀ values for Ub-I were measured to be about 10–140-fold lower than those for Compound I (Table 1), suggesting that the pre-formed adduct, Ub-I, can directly bind UAE to form a tight, inactive complex and inhibit its ATP-PP_i exchange activity (Fig. 1C). The difference observed in IC₅₀ values could result from different inhibition mechanisms

Substrate-assisted E1 Inhibition

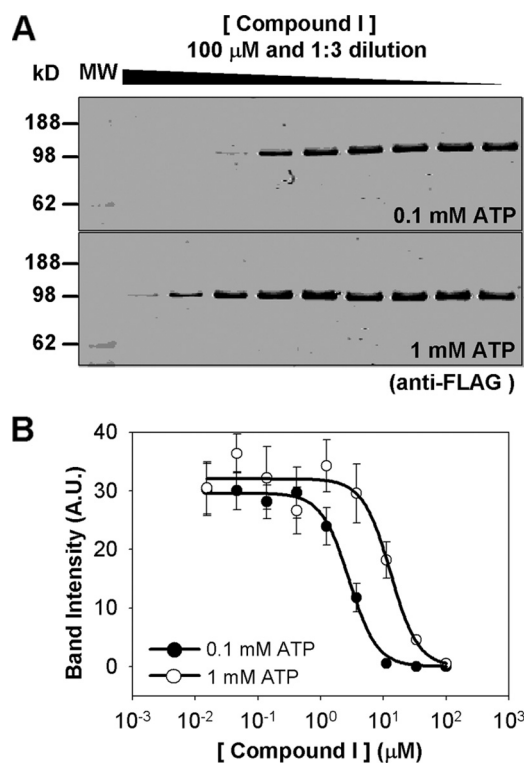


FIGURE 3. Inhibition of UAE-S~ubiquitin thioester by Compound I. *A*, Western blots showing dose-dependent loss of UAE-S~ubiquitin thioester with 0.1 mM ATP (*top panel*) or 1 mM ATP (*bottom panel*) using N-FLAG-ubiquitin as the substrate. Blots were probed with mouse anti-FLAG antibody. *B*, quantitation and data analysis of Western blots shown in *A*. The protein bands were visualized and quantitated using a fluorescently labeled secondary antibody (A.U., arbitrary fluorescence unit). IC_{50} values of 2.8 ± 0.2 and 12.9 ± 2.4 μ M were obtained with 0.1 mM ATP (*filled circles*) and 1 mM ATP (*open circles*), respectively. The concentration range of Compound I is from 0.15 to 100 μ M in a 3-fold dilution series.

(hence kinetics of inhibition) between Compound I and Ub-I (see the results and discussions in later sections). In addition, the proposed inhibition mechanism predicts that UAE-S~ubiquitin is no longer required for the pre-formed Ub-I adduct to bind and inhibit the ATP-PP_i exchange activity of UAE. Consistent with this hypothesis, Ub-I inhibited C632A UAE as well in an ATP-competitive fashion (Fig. 2*B* and Table 1). The ATP competitiveness of both Ub-I and Compound I inhibition reflects the ability of ATP to bind either apo-UAE to initiate step 1 (competing with Ub-I) or UAE-S~ubiquitin to initiate step 3 (competing with Compound I) (Fig. 1*A*).

Inhibition of UAE-S~Ubiquitin and E1-E2 Transthioylation by Compound I—Because Compound I is thought to bind and react with UAE-S~ubiquitin, loss of the thioester mediated by Compound I was directly assessed by SDS-PAGE followed by Western blot analysis using N-FLAG-ubiquitin. As shown in Fig. 3*A*, Compound I causes dose-dependent suppression of UAE-S~ubiquitin. Furthermore, the effect of Compound I on the level of UAE-S~ubiquitin appears to be ATP competitive, as increasing the ATP concentration from 0.1 to 1 mM raised the IC_{50} value from 2.8 ± 0.2 to 12.9 ± 2.4 μ M (Fig. 3*B*). This result is consistent with observed competitiveness of ATP in ATP-PP_i exchange assays. Consistent with the inhibition mechanism, formation of the N-FLAG-Ub-I adduct was also detected in the same reaction mixture, which shows similar

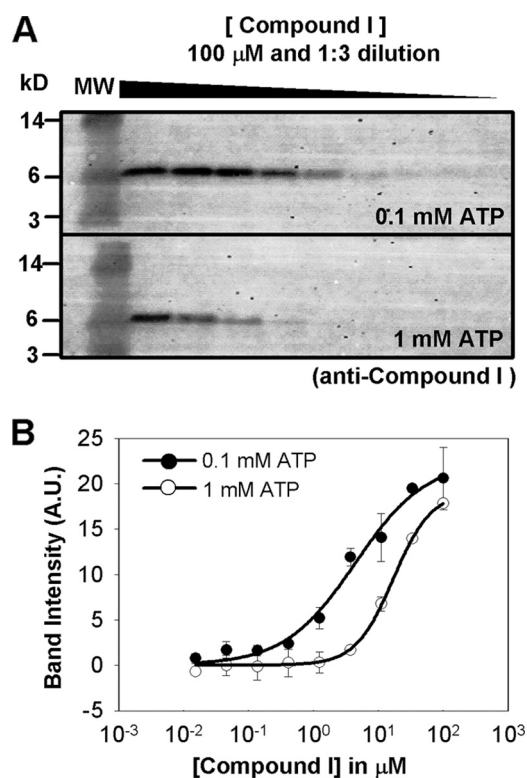


FIGURE 4. Ub-I adduct formation during the course of Compound I-mediated inhibition of UAE-S~ubiquitin thioester. *A*, Western blots showing dose-dependent formation of Ub-I with 0.1 mM ATP (*top panel*) or 1 mM ATP (*bottom panel*) using N-FLAG-ubiquitin as the substrate. Blots were probed with rabbit anti-Compound I antibody. *B*, quantitation and data analysis of Western blots shown in *A*. The protein bands were visualized and quantitated using a fluorescently labeled secondary antibody (A.U., arbitrary fluorescence unit). $K_{1/2}$ values of 4.4 ± 1.3 and 16.8 ± 1.1 μ M were obtained with 0.1 mM ATP (*filled circles*) and 1 mM ATP (*open circles*), respectively. The concentration range of Compound I is from 0.15 to 100 μ M in a 3-fold dilution series.

ATP competitiveness (Fig. 4*A*). The apparent $K_{1/2}$ values obtained from the dose-dependent adduct formation plots, 4.4 ± 1.3 (0.1 mM ATP) and 16.1 ± 1.1 μ M (1 mM ATP) (Fig. 4*B*), agree well with the observed IC_{50} values obtained in the thioester inhibition analysis (Fig. 3*B*).

In an attempt to further characterize the binding interaction between Compound I and UAE-S~ubiquitin, we performed ATP-AMP exchange assays. Unlike the ATP-PP_i exchange assay in which radioactive PP_i reacts with the adenylate intermediate in steps 1 or 3 (Fig. 1*A*), in ATP-AMP exchange assays, the UAE-S~ubiquitin intermediate is directly interrogated by monitoring its reaction with radiolabeled [³H]AMP to form ubiquitin adenylate (step 2) and subsequent conversion to ATP in the presence of PP_i (step 1) (11). The IC_{50} value obtained by titrating Compound I into the reaction mixture is thought to reflect direct competition between Compound I and AMP in binding to UAE-S~ubiquitin. Consistent with the hypothesis, the IC_{50} value obtained using the ATP-AMP exchange assay, 11.5 ± 1.4 μ M (supplemental Fig. S2), agrees relatively well with the IC_{50} value of 12.9 ± 2.4 μ M measured in the UAE-S~ubiquitin inhibition assay by Western blot analysis with the same ATP concentration (1 mM) (11).

To probe whether suppression of UAE-S~ubiquitin by Compound I also leads to inhibition of the subsequent E1-E2 transthioylation step, we also developed a proximity-based,

TABLE 2

Summary of quantitation of AMP/adenylate and PP_i release during UAE-mediated ubiquitin activation

	Ratio of AMP to UAE	Ratio of PP _i to UAE
WT UAE	1.96	2.04
WT UAE + Compound I	0.88	1.20
WT UAE + Ub-I	0.01	<0.01
C632A UAE	1.07	1.06

time-resolved fluorescence energy transfer assay to detect the E2-S~ubiquitin thioester using a similar strategy as described before with UbcH2 as the E2 (18). Both Compound I and Ub-I are potent inhibitors in this assay, with IC₅₀ of 1.4 ± 0.2 and 0.39 ± 0.1 nM, respectively (supplemental Fig. S3). Similar to that observed in ATP-PP_i exchange assays, Ub-I demonstrated a higher potency than Compound I, reflecting the different inhibition mechanisms and/or possible kinetics between the two inhibitors.

Quantitation of ATP Hydrolysis during UAE-mediated Ubiquitin Activation—To gain additional insight into the mechanism of E1 inhibition, we quantitated the amount of AMP or PP_i release in the ubiquitin-activation reactions using [α -³²P]- or [γ -³²P]ATP, respectively. Consistent with the proposed three-step mechanism (Fig. 1A) (11, 12), wild-type UAE was shown to catalyze 2 eq of ATP hydrolysis, generating 2 eq of AMP and PP_i (Table 2, the ubiquitin adenylate intermediate was converted to AMP during the analysis). C632A UAE, which is expected to catalyze the first ubiquitin adenylate formation but not subsequent step 2 and 3 reactions, only generated 1 eq of AMP and PP_i (Table 2). In the presence of Compound I, UAE-S~ubiquitin is proposed to be converted to the Ub-I adduct after step 2 and is unable to proceed to step 3 (Fig. 1A). Consistent with the mechanism, release of only 1 eq of AMP and PP_i was observed (Table 2). When Ub-I was included in the reaction mixture, no AMP or PP_i release was observed, suggesting an inactive UAE complex was formed before the first ATP hydrolysis (Table 2).

Time-dependent Inhibition of UAE by Compound I—Time-dependent inhibition of UAE by Compound I was assessed by progress curve analysis of its ATP-PP_i exchange activity. As shown in Fig. 5A, an apparent slow, tight binding inhibition pattern was observed for Compound I in the presence of 100 μ M ATP, which is similar to what was observed for MLN4924-mediated NAE inhibition (21). The observed rates of inactivation (k_{obs}) were obtained for each Compound I concentration by fitting the progress curves using a slow, tight-binding inhibition model (Fig. 5A) (23). By plotting k_{obs} versus Compound I concentration ($[I]$), we estimated the apparent $k_{obs}/[I]$ value to be $2.6 \pm 0.2 \times 10^4 \text{ M}^{-1} \text{ s}^{-1}$ (Fig. 5C, filled circles). This apparent second-order rate constant reflects the combined kinetic and binding parameters involved in the sequence of events leading to UAE inhibition, including the rate of UAE-S~ubiquitin formation, binding of Compound I to UAE-S~ubiquitin, and the rate of Ub-I formation. When a similar analysis was performed with 1 mM ATP, the apparent $k_{obs}/[I]$ was determined to be $3.3 \times 10^3 \text{ M}^{-1} \text{ s}^{-1}$, ~8-fold slower than that with 100 μ M ATP (data not shown). The negative influence of ATP on the kinetics of UAE inactivation is consistent with its competitive binding to UAE-S~ubiquitin, which, in turn, reduces the fraction of

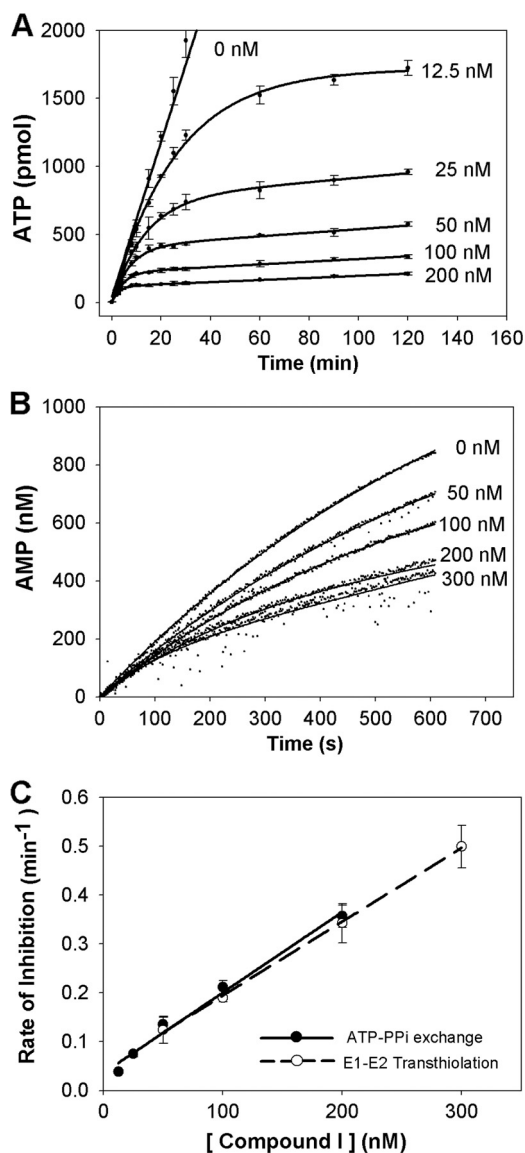


FIGURE 5. Time-dependent UAE inhibition demonstrated by progress curve analysis. A, time course of radioactive ATP production in ATP-PP_i exchange assays at various [Compound I]. B, time course of AMP production during UAE activation/UAE-UbcH10 transthiolation monitored using an ADT-ATP cycling system at various [Compound I]. For curves in A and B, the observed rate of inactivation (k_{obs}) was estimated by fitting the curves using a slow, tight-binding inhibition model: $Y = v_{bkg} \times t + A_0 \times (1 - \exp(-k_{obs} t))$. C, estimation of k_{inact}/K_i by linear fitting k_{obs} versus [Compound I]. Similar k_{inact}/K_i values were obtained in these two assays ($2.6 \pm 0.2 \times 10^4 \text{ M}^{-1} \text{ s}^{-1}$ from ATP-PP_i exchange assays and $2.5 \pm 0.2 \times 10^4 \text{ M}^{-1} \text{ s}^{-1}$ from transthiolation). The concentration of ATP in both assays is 0.1 mM.

UAE-S~ubiquitin that is available to bind Compound I and form a tight, inactive complex.

Time-dependent UAE inhibition was also studied in the E1-E2 transthiolation reaction by continuously monitoring AMP production using UbcH10 as the E2. This assay couples steady-state AMP release to loss of the NADH fluorescence signal due to its reduction using a myokinase-mediated ADP-ATP cycling system together with pyruvate kinase/lactate dehydrogenase (24). The rate of E1-E2 transthiolation can be quantitatively measured using this coupled assay with an observed rate of $1.98 \pm 0.02 \text{ s}^{-1}$ (supplemental Fig. S4). Compound I was demonstrated to inhibit E1-E2 transthiolation in a

Substrate-assisted E1 Inhibition

time-dependent fashion, similar to that observed in ATP-PP_i exchange assays (Fig. 5B). By plotting the observed rate of inactivation (k_{obs}) versus Compound I concentration, we obtained an apparent $k_{\text{obs}}/[I]$ value of $2.5 \pm 0.2 \times 10^4 \text{ M}^{-1} \text{ s}^{-1}$ (Fig. 5C, open circles), which is very similar to the one determined in ATP-PP_i exchange assays (Fig. 5C, filled circles) with the same ATP concentration (100 μM). This result suggests that binding of UbcH10 to UAE and subsequent transthiolation does not kinetically affect the rate-limiting step of UAE inactivation by Compound I.

Pre-steady-state Kinetic Analysis to Determine the Rate of Adduct Formation—To study binding of Compound I to UAE-S~ubiquitin and the rate of Ub-I formation directly, we performed pre-steady-state single turnover kinetic analysis by mixing pre-formed UAE-S~ubiquitin with Compound I and quantitating the rate of Ub-I formation on a millisecond time scale. Pre-formed UAE-S~ubiquitin was obtained by reacting an excess amount of UAE with ubiquitin and Mg^{2+} -ATP and the resulting mixture was desalted to remove small molecule components. Under such a condition, we expected that most of the UAE-S~ubiquitin would not bind a second ubiquitin or ATP molecule because of the limiting amount of ubiquitin (13). The desalted sample contained about 2 μM UAE-S~ubiquitin assuming 100% conversion. We expected the actual concentration to be lower than 2 μM due to the efficiency of the reaction, degradation of UAE-S~ubiquitin, and formation of the ternary complex. Therefore, the final sample contained a mixed population of UAE consisting of unreacted UAE, UAE-S~ubiquitin, and the ternary complex. However, the exact concentration of pre-formed UAE-S~ubiquitin is not critical to the subsequent kinetic analysis because other UAE species were not expected to interact with Compound I based on previous biochemical and biophysical studies (21, 22). In addition, once formed, Ub-I binds tightly to UAE, which renders the reaction between UAE-S~ubiquitin and Compound I inherently a single turnover. The UAE-S~ubiquitin sample (with a calculated concentration of 1 μM after mixing) was then rapidly mixed with Compound I using a chemical quench apparatus and the amounts of Ub-I formed were determined by quantitative Western analysis using a standard curve generated with the purified Ub-I adduct. Under this condition, a first-order kinetic profile was observed for each Compound I concentration (supplemental Fig. S5). The apparent rate constant (k_{obs}) was then plotted versus Compound I concentration and the data were fitted to obtain the maximum rate of inactivation (k_{inact}) and the inhibition constant (K_i) using the equation: $k_{\text{obs}} = k_{\text{inact}} \times [\text{Compound I}] / ([\text{Compound I}] + K_i)$. Fig. 6 shows that formation of Ub-I occurs with k_{inact} of $8.3 \pm 0.7 \text{ s}^{-1}$ and K_i of $27 \pm 6 \mu\text{M}$. Based on the amount of Ub-I formed at the end of the reaction, we estimated that about 50% of the total UAE species existed as UAE-S~ubiquitin in the final reaction mixture ($\sim 0.5 \mu\text{M}$). The k_{inact}/K_i value determined under this condition in the absence of ATP, $3.1 \times 10^5 \text{ M}^{-1} \text{ s}^{-1}$, is about 12-fold higher than the $k_{\text{obs}}/[I]$ value obtained from the progress curve analysis with 100 μM ATP ($2.6 \times 10^4 \text{ M}^{-1} \text{ s}^{-1}$) or 90-fold higher than the one with 1 mM ATP ($3.3 \times 10^3 \text{ M}^{-1} \text{ s}^{-1}$). Therefore, the single-turnover analysis using a pre-formed UAE thioester allowed us to study the key step of Ub-I formation without competition from ATP.

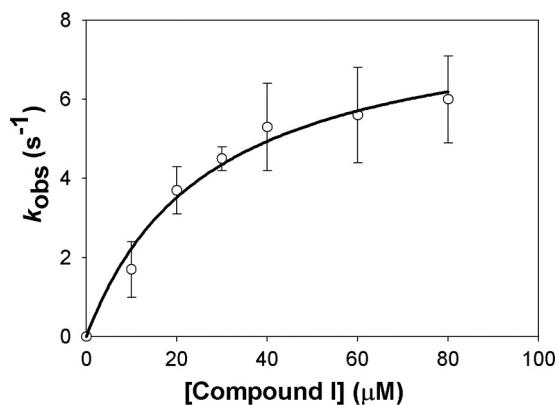


FIGURE 6. Determination of the rate of Ub-I formation under single-turnover conditions. The observed rates (k_{obs}) were plotted versus [Compound I]. K_i ($27 \pm 6 \mu\text{M}$) and k_{inact} ($8.3 \pm 0.7 \text{ s}^{-1}$) were obtained by fitting the data to a hyperbolic equation: $k_{\text{obs}} = k_{\text{inact}} \times [\text{Compound I}] / ([\text{Compound I}] + K_i)$.

Ub-I Forms a Tight Complex with UAE—Crystallographic studies revealed that the NEDD8-MLN4924 adduct forms a complex with NAE by binding at both the NEDD8- and nucleotide-binding pockets and prevents NAE from binding either ATP or NEDD8 (21). In the present study, the purified Ub-I adduct allowed us to examine its binding affinity with UAE directly. SPR analysis showed that, in the absence of ATP, Ub-I binds UAE with an association rate (k_a) of $1.9 \times 10^6 \text{ M}^{-1} \text{ s}^{-1}$ and a dissociation rate (k_d) of $<1 \times 10^{-4} \text{ s}^{-1}$ (Fig. 7). This result suggests that the dissociation constant (K_D or k_d/k_a) is less than 50 pM for the UAE·Ub-I complex. The k_a values also decreased with an increasing ATP concentration (Table 3), which is consistent with ATP-competitive inhibition by Ub-I (Table 1). The fast association rate of Ub-I ($1.09 \times 10^6 \text{ M}^{-1} \text{ s}^{-1}$) compared with the observed rate of inactivation for Compound I ($k_{\text{obs}}/[I]$: $2.6 \times 10^4 \text{ M}^{-1} \text{ s}^{-1}$) under similar conditions (100 μM ATP) could explain the observed potency difference between Ub-I and Compound I in ATP-PP_i exchange assays (5.0 and 91 nM for Ub-I and Compound I, respectively). As a comparison, ubiquitin alone showed weak affinity to UAE by SPR and ITC studies (supplemental Fig. S6). One-site model analysis of the equilibrium binding signals of SPR suggests that the K_D for ubiquitin is $10.3 \pm 4.7 \mu\text{M}$ (supplemental Fig. S6, A and B), which is consistent with the result from ITC studies (K_D , $12.0 \pm 4.6 \mu\text{M}$; N, 1.01 ± 0.05) (supplemental Fig. S6C).

To assess the effect of the slow dissociation rate on the enzymatic activity of UAE, we performed UAE activity recovery assays. The UAE·Ub-I complex was pre-formed by mixing UAE with ubiquitin, ATP, and Compound I. The resulting mixture was desalted and diluted so that the complex concentration was below the apparent IC_{50} ($\sim 20 \text{ pM}$). The recovery of UAE activity was assessed by measuring the E1-E2 transthiolation activity of UAE using the fluorescence energy transfer assay as described above. As shown under supplemental Fig. S7, in the presence of 3 mM ATP, about 10% UAE activity was recovered in 4 h, suggesting that k_d is $\sim 1.6 \times 10^{-4} \text{ s}^{-1}$. The recovery assay result agrees with the one obtained in SPR studies and further supports stable complex formation between UAE and Ub-I.

Inhibition of UAE by MLN4924 and Ub-4924 Adduct—MLN4924, which shows potent and selective inhibition against NAE, is a relatively weak inhibitor of UAE (IC_{50} , $12.0 \pm 1.6 \text{ nM}$

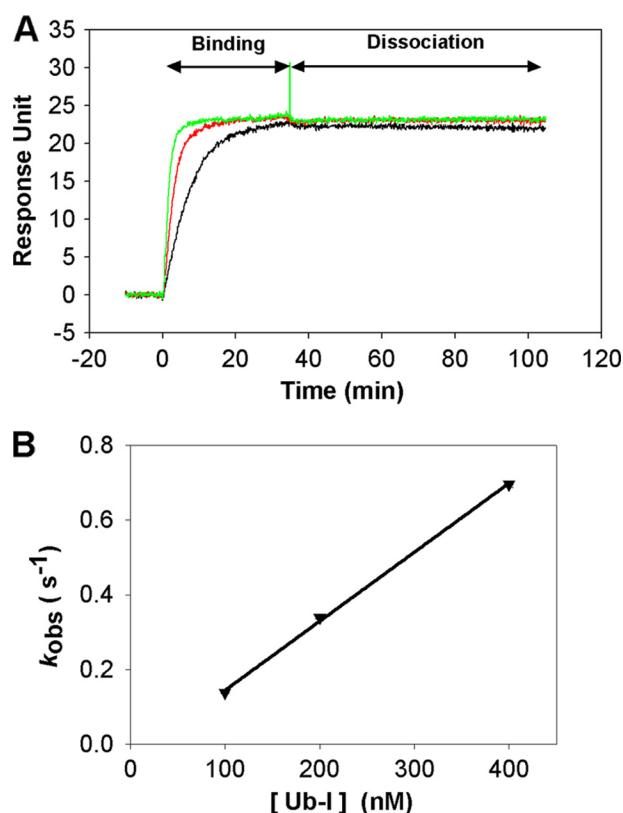


FIGURE 7. Binding interaction between UAE and Ub-I studied by surface plasmon resonance. *A*, sensorgrams of Ub-I (0.1, 0.2, and 0.4 μM , black, red, and green traces, respectively) binding to UAE immobilized on the sensor chip surface. The binding phase of the data were fit to a single-exponential rise to derive apparent association rates (k_{obs}). No measurable dissociation was observed during the course of experiments. *B*, k_{obs} was plotted against [Ub-I] to obtain the association rate (k_a) of $1.9 \times 10^6 \text{ M}^{-1} \text{ s}^{-1}$.

TABLE 3

Association rates of Ub-I binding to UAE with different ATP concentrations determined by SPR

	0 μM ATP	50 μM ATP	100 μM ATP	200 μM ATP
$k_a (\times 10^6 \text{ M}^{-1} \text{ s}^{-1})$	1.85 ± 0.06	1.79 ± 0.07	1.09 ± 0.03	0.73 ± 0.01

for NAE and $22.1 \pm 5.8 \mu\text{M}$ for UAE in the ATP-PP_i exchange assay with 0.1 mM ATP) (supplemental Fig. S8A). In addition, the progress curve analysis showed that the observed rate of UAE inhibition was less than $1 \times 10^{-4} \text{ s}^{-1}$ with 5 μM MLN4924 ($k_{\text{obs}}/[\text{MLN4924}] < 20 \text{ M}^{-1} \text{ s}^{-1}$, compared with $3.3 \times 10^3 \text{ M}^{-1} \text{ s}^{-1}$ for Compound I with 1 mM ATP) (data not shown), suggesting that weak compound binding and/or slow adduct formation might be responsible for the observed weak potency. Consistent with this hypothesis, the purified ubiquitin-MLN4924 adduct (Ub-4924), which could be obtained by incubating UAE, ubiquitin, and ATP with MLN4924, demonstrated higher potency against UAE (IC_{50} , $1.6 \pm 0.8 \mu\text{M}$) than the free compound (IC_{50} , $22.1 \pm 5.8 \mu\text{M}$) (supplemental Fig. S8B). However, Ub-4924 (IC_{50} , $1.6 \pm 0.8 \mu\text{M}$) was still much less potent than Ub-I (IC_{50} , $5.0 \pm 0.5 \text{ nM}$) under similar assay conditions (supplemental Fig. S8B). Furthermore, no inhibitory effect was observed for Ub-4924 (up to 0.8 μM) when NAE was used in the E1 activity assay (supplemental Fig. S8C, open circles), suggesting that both Ubl and the compound moieties are critical to

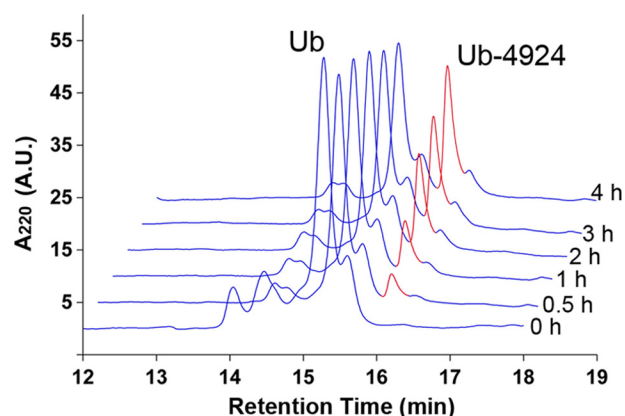


FIGURE 8. Steady-state formation of the UAE-catalyzed ubiquitin-MLN4924 (Ub-4924) adduct analyzed by reverse-phase HPLC. Peaks corresponding to Ub-4924 are highlighted in red. The area under the Ub-4924 peaks were integrated and converted to the amount of Ub-4924 using a purified sample as a standard, which yielded a steady-state rate of $1.4 \times 10^{-3} \text{ s}^{-1}$ or $\sim 5 \text{ h}^{-1}$.

E1-selective inhibition mediated by a Ubl-adenosine sulfamate adduct.

Fast Dissociation Rate of Ub-4924 Contributes to Its Weak Inhibition against UAE—To assess the affinity of Ub-4924 and UAE directly, we performed SPR analysis on the purified Ub-4924 adduct as described for Ub-I. The Ub-4924 adduct showed a dissociation rate of $1.1 \times 10^{-2} \text{ s}^{-1}$, more than 100 times faster than Ub-I ($< 1 \times 10^{-4} \text{ s}^{-1}$) (supplemental Fig. S9). In addition, the UAE activity recovery assay showed that the pre-formed Ub-4924-UAE complex regained activity at a similar rate as the DMSO control (supplemental Fig. S7). These results suggest that Ub-4924 does not form a tight complex with UAE and that dissociation of Ub-4924 allows rapid recovery of UAE activity in the presence of ATP and ubiquitin. Consistent with these results, we found that UAE catalyzed multiple cycles of Ub-4924 production with an estimated steady-state rate of 5 h^{-1} , or $1.4 \times 10^{-3} \text{ s}^{-1}$ (Fig. 8). From this aspect, MLN4924 acts as a substrate for UAE. The steady-state rate of Ub-4924 formation reflects the rate-limiting step of the catalytic cycle, which could be the rate of Ub-4924 formation or the rate of adduct release under the assay conditions. Therefore, the potency of adenosine sulfamate analogues in inhibition of E1s is affected not only by the rate of adduct formation, but also by the affinity between the adduct and E1.

Inhibition of Ubiquitination in HCT116 Cells by Compound I—Compound I also inhibits UAE-mediated polyubiquitination in a cellular setting. When HCT116 cells (a human colon cancer cell line) were treated with 10 μM Compound I for 1 h, loss of polyubiquitinated protein substrates was observed by Western blot analysis compared with DMSO-treated cells (Fig. 9, middle panel). Furthermore, loss of UbcH10-S~ubiquitin thioester was also detected (top panel), which is entirely consistent with the inhibition of UAE-UbcH10 transthiolation observed in progress curve analysis (Fig. 5, B and C). Because Compound I also inhibited other E1s in biochemical assays (supplemental Table S1), the cellular outcomes of Compound I treatment are expected to be pleiotropic due to its potential impact on diverse biological pathways regulated by different E1s. Detailed studies are underway to understand cellular responses caused by Com-

Substrate-assisted E1 Inhibition

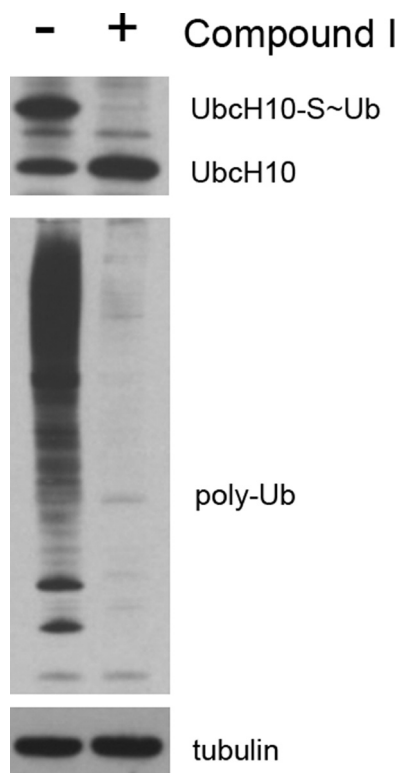


FIGURE 9. Western blot analysis demonstrating the ubiquitination pathway inhibition in Compound I-treated cells. HCT116 cells were treated with DMSO or 10 μM Compound I for 1 h. The cells were then harvested and whole cell extracts were subjected to SDS-PAGE and Western blot analysis under nonreducing conditions. *Upper panel*, anti-UbH10; *middle panel*, anti-ubiquitin; *bottom panel*, anti-tubulin.

Compound I and other more selective adenosine sulfamate analogues and will be presented in future communications.

DISCUSSION

UAE and other E1s activate their cognate UbIs via a UbI-adenylate intermediate and initiate an enzymatic cascade that ultimately conjugates ubiquitin and UbIs to targeted substrates. Given the conserved UbI-activation process exhibited by all E1s (10, 14), the mechanism-based E1 inhibition mediated by adenosine sulfamate analogues first discovered for MLN4924 and NAE could also be observed in other E1 systems (21). In the current study, we presented biochemical studies that demonstrated potent inhibition of UAE by Compound I, an adenosine sulfamate analogue (Fig. 1B). Compound I inhibited UAE-dependent ATP-PP_i exchange activity (Fig. 2), caused loss of UAE-S~ubiquitin thioester (Fig. 3), and inhibited E1-E2 transthiolation (Fig. 5B and supplemental Fig. S3) in a dose-dependent manner. The species that was proposed to be responsible for UAE inhibition, a covalent ubiquitin-Compound I adduct (Ub-I) similar to the NEDD8-MLN4924 adduct, was identified by mass spectroscopic analysis of the inhibition reaction mixture (21) and was isolated for biochemical characterization (supplemental Fig. S1). Ub-I potentially inhibited the ATP-PP_i exchange activity of UAE and E1-E2 transthiolation (Fig. 2 and supplemental Fig. S3). In addition, Ub-I was shown to form a tight complex for UAE with $K_D < 50$ pM in SPR studies (Fig. 7), similar to what has been estimated for the ubiquitin adenylate

($K_D < 8$ pM) (25). These results strongly suggest that Ub-I mimics the ubiquitin adenylate intermediate and binds at the active site of UAE to prevent further recruitment of substrates.

The covalent adduct-forming mechanism we hypothesize for E1 inhibition by adenosine sulfamates is entirely consistent with the three-step ubiquitin activation process first proposed for UAE by Haas *et al.* (11, 12). Inhibition of the enzymatic activity of UAE by Compound I is strictly dependent on the catalytic cysteine residue (Cys⁶³²), suggesting that UAE-S~ubiquitin is the required intermediate leading to Ub-I formation (Fig. 2B). Consistent with this observation, the purified Ub-I adduct, which circumvents the adduct forming step, inhibits both wild-type and C632A UAE (Fig. 2). To further support the proposed mechanism of UAE inhibition via Ub-I adduct formation, we quantitated the amount of ATP hydrolyzed by UAE during ubiquitin activation in the absence and presence of inhibitors. As proposed by Haas *et al.* (12) (Fig. 1A), without ubiquitin-conjugating enzymes (E2), UAE is thought to undergo one cycle of the three-step ubiquitin activation, consuming 2 eq of ATP and generating 2 eq of AMP-containing species (1 eq of free AMP and 1 eq of ubiquitin adenylate), concomitantly releasing 2 eq of PP_i (Fig. 1A). In the presence of Compound I, hydrolysis of only 1 eq of ATP was observed, compared with no ATP hydrolysis with Ub-I (Table 2). These results are consistent with Compound I reacting with UAE-S~ubiquitin, which occurs after the first ATP hydrolysis, whereas Ub-I is capable of binding apo-E1, thereby inhibiting ATP binding and hydrolysis all together.

Two distinct conformations, open and closed, have been proposed for E1s during the UbI-activation cycle. Most structural studies on E1s with a distinct catalytic cysteine domain revealed a distance of ~ 25 – 30 Å between the catalytic cysteine residue and the nucleotide binding pocket, which represents an “open” conformation (26–29). The open conformation is thought to be required for binding UbI and Mg²⁺-ATP in steps 1 and 3 (28, 29). However, in step 2, the long distance in the open conformation has to be overcome in order for the catalytic Cys to initiate nucleophilic attack of the ubiquitin adenylate located in the nucleotide binding pocket. Recent x-ray crystallographic studies of small ubiquitin-like modifier (SUMO)-activating enzyme revealed a “closed” conformation in which the catalytic cysteine residue formed a covalent, tetrahedral intermediate with a SUMO 5'-vinylsulfonylamino deoxy adenylate analogue in the nucleotide binding pocket (30). Interestingly, in our study, no apparent affinity was observed between Compound I and apo-UAE (data not shown), which is presumably in the open conformation based on previous structural studies (26). We believe that Compound I binds to UAE-S~ubiquitin in a conformation that either mimics or can transition to a closed conformation in which the nucleophilic attack of UAE-S~ubiquitin by Compound I likely occurs (Fig. 1C), a conformation that probably resembles what was observed for SUMO-activating enzyme with a covalently trapped intermediate (30). This process is similar to the reverse reaction of step 2 where AMP serves as the nucleophile (Fig. 1A). Furthermore, our results suggest that UAE-S~ubiquitin most likely undergoes rapid equilibrium among different conformations, because ATP, which is thought to bind selectively to the open conformation

(30), competes effectively with Compound I-mediated inhibition and adduct formation (Table 1 and Figs. 3 and 4).

Pre-steady-state kinetic studies under single-turnover conditions provide additional insight into the adduct forming reaction between Compound I and UAE-S~ubiquitin. The rate constant (k_{inact}) obtained in this study, $8.3 \pm 0.7 \text{ s}^{-1}$, reflects a rate-limiting step leading to Ub-I formation. It could be the conformational change that allows the catalytic cysteine domain to position ubiquitin thioester to the proximity of Compound I or the actual chemical step of nucleophilic attack by the amino group in Compound I. To place this rate constant in the context of the three-step ubiquitin-activation process, we also measured the rates of ubiquitin-adenylate formation (step 1) and UAE-S~ubiquitin formation (step 2) directly by rapid chemical quench on a millisecond to second time scale. In the absence of E2, UAE can only catalyze one cycle of ATP hydrolysis/adenylate formation under ubiquitin-limiting conditions, resulting in a single-turnover kinetic process. The observed adenylation rate was $\sim 18.8 \pm 2.2 \text{ s}^{-1}$, which was about 4 times faster than the rate of UAE-S~ubiquitin formation ($4.3 \pm 0.8 \text{ s}^{-1}$) under similar single turnover conditions (supplemental Fig. S10). These observed rates agree well with previous studies (11, 31) and suggest that UAE-S~ubiquitin formation is the rate-limiting step in ubiquitin activation (31). Although the intrinsic rate of Ub-I formation, $8.3 \pm 0.7 \text{ s}^{-1}$, is about twice as fast as the rate of UAE-S~ubiquitin formation, under physiological conditions of $\sim 1 \text{ mM}$ ATP, the rate was estimated to decrease significantly to $\sim 0.1 \text{ s}^{-1}$, making adduct formation the rate-limiting step in the entire UAE inhibition process.

Human E1 family members share structural similarity and are proposed to use a common mechanism to activate UbIs. However, many residues in their nucleotide binding domain are not conserved, which leads to distinct spatial arrangement of amino acid side chains that are in close proximity to ATP (26–29, 32). The striking selectivity of MLN4924 toward NAE suggests that the adenosine sulfamate scaffold can be tailored to specifically inhibit individual E1 enzymes. The current work shows that both the rate of adduct formation and the affinity between Ubl-inhibitor adduct and E1 contribute to the overall potency of inhibition. Thus, a complex structure-activity relationship must be considered in developing novel therapeutics that selectively target each E1 pathway.

Acknowledgments—We thank M. Bembenek and J. Yan for technical help with adduct and E1 thioester quantitation, A. Burkhardt for developing compound-specific antibodies, T. Soucy, H. Liao, B. Amidon, and F. Melandri for helpful discussions, and J. Bolen for support and guidance.

REFERENCES

- Balch, W. E., Morimoto, R. I., Dillin, A., and Kelly, J. W. (2008) *Science* **319**, 916–919
- Cohen, F. E., and Kelly, J. W. (2003) *Nature* **426**, 905–909
- Mu, T. W., Ong, D. S., Wang, Y. J., Balch, W. E., Yates, J. R., 3rd, Segatori, L., and Kelly, J. W. (2008) *Cell* **134**, 769–781
- Kane, R. C., Bross, P. F., Farrell, A. T., and Pazdur, R. (2003) *Oncologist* **8**, 508–513
- Kane, R. C., Dagher, R., Farrell, A., Ko, C. W., Sridhara, R., Justice, R., and Pazdur, R. (2007) *Clin. Cancer Res.* **13**, 5291–5294
- Nalepa, G., Rolfe, M., and Harper, J. W. (2006) *Nat. Rev. Drug Discov.* **5**, 596–613
- Hoeller, D., Hecker, C. M., and Dikic, I. (2006) *Nat. Rev. Cancer* **6**, 776–788
- Hoeller, D., and Dikic, I. (2009) *Nature* **458**, 438–444
- Bedford, L., Lowe, J., Dick, L. R., Mayer, R. J., and Brownell, J. E. (2011) *Nat. Rev. Drug Discov.* **10**, 29–46
- Schulman, B. A., and Harper, J. W. (2009) *Nat. Rev. Mol. Cell Biol.* **10**, 319–331
- Haas, A. L., and Rose, I. A. (1982) *J. Biol. Chem.* **257**, 10329–10337
- Haas, A. L., Warms, J. V., Hershko, A., and Rose, I. A. (1982) *J. Biol. Chem.* **257**, 2543–2548
- Pickart, C. M., Kasperek, E. M., Beal, R., and Kim, A. (1994) *J. Biol. Chem.* **269**, 7115–7123
- Streich, F. C., Jr., and Haas, A. L. (2010) *Subcell. Biochem.* **54**, 1–16
- Liakopoulos, D., Doenges, G., Matuschewski, K., and Jentsch, S. (1998) *EMBO J.* **17**, 2208–2214
- Osaka, F., Kawasaki, H., Aida, N., Saeki, M., Chiba, T., Kawashima, S., Tanaka, K., and Kato, S. (1998) *Genes Dev.* **12**, 2263–2268
- Bohnsack, R. N., and Haas, A. L. (2003) *J. Biol. Chem.* **278**, 26823–26830
- Soucy, T. A., Smith, P. G., Milhollen, M. A., Berger, A. J., Gavin, J. M., Adhikari, S., Brownell, J. E., Burke, K. E., Cardin, D. P., Critchley, S., Cullis, C. A., Doucette, A., Garnsey, J. J., Gaulin, J. L., Gershman, R. E., Lublinsky, A. R., McDonald, A., Mizutani, H., Narayanan, U., Olhava, E. J., Peluso, S., Rezaei, M., Sintchak, M. D., Talreja, T., Thomas, M. P., Traore, T., Vyskocil, S., Weatherhead, G. S., Yu, J., Zhang, J., Dick, L. R., Claiborne, C. F., Rolfe, M., Bolen, J. B., and Langston, S. P. (2009) *Nature* **458**, 732–736
- Soucy, T. A., Smith, P. G., and Rolfe, M. (2009) *Clin. Cancer Res.* **15**, 3912–3916
- Milhollen, M. A., Traore, T., Adams-Duffy, J., Thomas, M. P., Berger, A. J., Dang, L., Dick, L. R., Garnsey, J. J., Koenig, E., Langston, S. P., Manfredi, M., Narayanan, U., Rolfe, M., Staudt, L. M., Soucy, T. A., Yu, J., Zhang, J., Bolen, J. B., and Smith, P. G. (2010) *Blood* **116**, 1515–1523
- Brownell, J. E., Sintchak, M. D., Gavin, J. M., Liao, H., Bruzzese, F. J., Bump, N. J., Soucy, T. A., Milhollen, M. A., Yang, X., Burkhardt, A. L., Ma, J., Loke, H. K., Lingaraj, T., Wu, D., Hamman, K. B., Spelman, J. J., Cullis, C. A., Langston, S. P., Vyskocil, S., Sells, T. B., Mallerer, W. D., Visiers, I., Li, P., Claiborne, C. F., Rolfe, M., Bolen, J. B., and Dick, L. R. (2010) *Mol. Cell* **37**, 102–111
- Bruzzese, F. J., Tsu, C. A., Ma, J., Loke, H. K., Wu, D., Li, Z., Tayber, O., and Dick, L. R. (2009) *Anal. Biochem.* **394**, 24–29
- Morrison, J. F., and Walsh, C. T. (1988) *Adv. Enzymol. Relat. Areas Mol. Biol.* **61**, 201–301
- Valero, E., Varón, R., and García-Carmona, F. (2000) *Biochem. J.* **350**, 237–243
- Burch, T. J., and Haas, A. L. (1994) *Biochemistry* **33**, 7300–7308
- Lee, I., and Schindelin, H. (2008) *Cell* **134**, 268–278
- Lois, L. M., and Lima, C. D. (2005) *EMBO J.* **24**, 439–451
- Walden, H., Podgorski, M. S., Huang, D. T., Miller, D. W., Howard, R. J., Minor, D. L., Jr., Holton, J. M., and Schulman, B. A. (2003) *Mol. Cell* **12**, 1427–1437
- Walden, H., Podgorski, M. S., and Schulman, B. A. (2003) *Nature* **422**, 330–334
- Olsen, S. K., Capili, A. D., Lu, X., Tan, D. S., and Lima, C. D. (2010) *Nature* **463**, 906–912
- Tokgöz, Z., Bohnsack, R. N., and Haas, A. L. (2006) *J. Biol. Chem.* **281**, 14729–14737
- Bacik, J. P., Walker, J. R., Ali, M., Schimmer, A. D., and Dhe-Paganon, S. (2010) *J. Biol. Chem.* **285**, 20273–20280